2000

Significance of anaerobic methane oxidation in methane-rich sediments overlying the Blake Ridge gas hydrates

Walter S. Borowski
Eastern Kentucky University, w.borowski@eku.edu

Tori M. Hoehler
NASA Ames Research Center

Mark J. Alperin
University North Carolina

Namcy M. Rodriguez
Shell

Charles K. Paull
MBARI

Paull, C.K., Matsumoto, R., Wallace, P.J., and Dillon, W.P. (Eds.), 2000
Proceedings of the Ocean Drilling Program, Scientific Results, Vol. 164

9. SIGNIFICANCE OF ANAEROBIC METHANE OXIDATION IN METHANE-RICH SEDIMENTS OVERLYING THE BLAKE RIDGE GAS HYDRATES[1]

Walter S. Borowski,[2,3] Tori M. Hoehler,[4,5] Marc J. Alperin,[4] Nancy M. Rodriguez,[2,3] and Charles K. Paull[2,6]

ABSTRACT

A unique set of geochemical pore-water data, characterizing the sulfate reduction and uppermost methanogenic zones, has been collected at the Blake Ridge (offshore southeastern North America) from Ocean Drilling Program (ODP) Leg 164 cores and piston cores. The $\delta^{13}C$ values of dissolved CO_2 (ΣCO_2) are as ^{13}C-depleted as –37.7‰ PDB (Site 995) at the sulfate-methane interface, reflecting a substantial contribution of isotopically light carbon from methane. Although the geochemical system is complex and difficult to fully quantify, we use two methods to constrain and illustrate the intensity of anaerobic methane oxidation in Blake Ridge sediments. An estimate using a two-component mixing model suggests that ~24% of the carbon residing in the ΣCO_2 pool is derived from biogenic methane. Independent diagenetic modeling of a methane concentration profile (Site 995) indicates that peak methane oxidation rates approach 0.005 µmol cm^{-3} yr^{-1}, and that anaerobic methane oxidation is responsible for consuming ~35% of the total sulfate flux into the sediments. Thus, anaerobic methane oxidation is a significant biogeochemical sink for sulfate, and must affect interstitial sulfate concentrations and sulfate gradients.

Such high proportions of sulfate depletion because of anaerobic methane oxidation are largely undocumented in continental rise sediments with overlying oxic bottom waters. We infer that the additional amount of sulfate depleted through anaerobic methane oxidation, fueled by methane flux from below, causes steeper sulfate gradients above methane-rich sediments. Similar pore water chemistries should occur at other methane-rich, continental-rise settings associated with gas hydrates.

INTRODUCTION

Sulfate reduction refers to microbially mediated diagenetic processes that deplete sulfate within interstitial pore waters. In anoxic marine sediments, sulfate reduction is generally the most important remineralization process (e.g., Reeburgh, 1983), with the net reaction adding dissolved carbon dioxide (ΣCO_2, or dissolved inorganic carbon, DIC) and sulfide to pore waters. Sulfate depletion typically occurs when microbes utilize interstitial sulfate that is ultimately derived from overlying seawater, to oxidize sedimentary organic matter (SOM) in the net reaction:

$$2\,(CH_2O) + SO_4^{2-} \rightarrow 2\,HCO_3^- + H_2S, \quad (1)$$

which also releases ammonium and phosphate to pore waters as net by-products of SOM degradation (Richards, 1965). An additional sink for sulfate occurs near the base of the sulfate reduction zone, or sulfate-methane interface (SMI), in a net process called anaerobic methane oxidation (AMO):

$$CH_4 + SO_4^{2-} \rightarrow HCO_3^- + HS^- + H_2O \quad (2)$$

(Reeburgh, 1976). Although sulfate and methane are apparently co-consumed in the net reaction, the pathway for this process is controversial (e.g., Hoehler et al., 1994).

In most marine sediments, oxidation of SOM (Eq. 1) is the predominant reaction that controls interstitial sulfate concentrations and gradients. However, in methane-charged sediments like those overlying gas hydrate deposits, AMO may become an important process that affects interstitial sulfate concentration gradients. Borowski et al. (1996) linked interstitial sulfate depletion in Carolina Rise and Blake Ridge (CR-BR) (offshore southeastern United States) sediments to upward methane flux and underlying methane inventory. In such methane-rich settings, AMO potentially consumes a significant portion of the interstitial sulfate pool, depleting sulfate more rapidly than oxidation of SOM alone. The underlying methane concentrations regulate the upward methane flux (usually through diffusion) and thus also control the rate of AMO. Steep sulfate gradients (and perhaps their linearity) and shallow depths to the sulfate-methane interface are a consequence of the increased influence of AMO within these continental rise sediments (Borowski, 1998).

We analyze geochemical evidence from Ocean Drilling Program (ODP) drilling on the Blake Ridge (Leg 164) to assess the importance of AMO as a mechanism influencing sulfate depletion. The data presented here are unique because of high-resolution sampling (~1- to 1.5-m intervals) through the upper methanogenic zone and entire sulfate reduction zone. The results substantiate inferences drawn from measurement of sulfate gradients in sediments collected previously by piston coring (Borowski et al., 1996, 1997; Borowski, 1998). Sulfate gradients are steep (and linear) within these methane-rich, continental-rise sediments, and supporting concentration and isotopic data used in simple mixing and diagenetic models demonstrate that AMO is a significant sink for sulfate. We infer that such a magnified role for AMO influences the magnitude and shapes of sulfate gradients in other marine, methane-rich settings associated with gas hydrates.

PREVIOUS WORK

Previous interstitial chemical data from Blake Ridge sediments are available from Deep Sea Drilling Project (DSDP) Leg 11 (Sites

[1]Paull, C.K., Matsumoto, R., Wallace, P.J., and Dillon, W.P. (Eds.), 2000. *Proc. ODP, Sci. Results,* 164: College Station, TX (Ocean Drilling Program).
[2]Geology Department, University of North Carolina at Chapel Hill, Chapel Hill, NC 27599-3315, U.S.A.
[3]Present address: Exxon Exploration Company, P.O. Box 4778, Houston, TX 77210-47778, U.S.A. Correspondence author: borowski@lcc.net
[4]Marine Sciences, University of North Carolina at Chapel Hill, Chapel Hill, NC 27599-3300, U.S.A.
[5]Present address: NASA Ames Research Center, MS 239-4, Moffett Field, CA 94035-1000, U.S.A. thoehler@mail.arc.nasa.gov
[6]Present address: Monterey Bay Aquarium Research Institute, 7700 Sandholdt Road, Moss Landing, CA 95039-0628, U.S.A.

102, 103, and 104; Hollister, Ewing, et al., 1972), from DSDP Site 533 (Leg 76, Sheridan, Gradstein, et al., 1983), and from 87 piston cores taken over the Blake Ridge and Carolina Rise (Borowski et al., 1996, 1997) (Fig. 1).

Three sites drilled on Leg 11 form a transverse transect on the Blake Ridge (Fig. 1) over prominent bottom-simulating reflectors (BSRs). The BSRs suggest the presence of gas hydrates in the subsurface (Lancelot and Ewing, 1972; Shipley et al., 1979). Moreover, although interstitial data from this leg are sparse, chloride data show strong downward freshening (Sayles et al., 1972; Presley and Kaplan, 1972), also suggesting gas hydrates are contained within the sediments (Hesse and Harrison, 1981). Sulfate data indicate that shallow sulfate-methane interfaces occur between 6 and 45 mbsf.

Site 533 was also drilled over a strong BSR, and interstitial chemical data show downward-freshening chloride profiles and ^{18}O-enrichments in pore waters (Jenden and Gieskes, 1983), indicating the presence of gas hydrates (Hesse and Harrison, 1981; Davidson et al., 1983). Sulfate data are insufficient to fully document the shape of the concentration profile, but sulfate is depleted between 9.8 and 14.4 mbsf (Claypool and Threlkeld, 1983). Methane and CO_2 data were used to identify large ^{13}C depletions of carbon in the dissolved CO_2 ($\delta^{13}C_{\Sigma CO_2}$ = –31.4‰ at 14.4 mbsf; Claypool and Threlkeld, 1983) and methane ($\delta^{13}C_{CH_4}$ = –91.3‰ at 33.9 mbsf; Galimov and Kvenvolden, 1983) pools, but did not provide isotopic data through the SMI.

Sulfate gradients at nondiapir sites over the CR-BR gas hydrate field are linear and vary by sixteenfold over the area as shown by piston coring (see fig. 1 in Borowski et al., 1996; fig. 2.1 in Borowski, 1998). However, the sulfate-methane interface was penetrated by only one piston core (PC 11–8; Fig. 1), where the depth to the sulfate-methane interface is 10.3 mbsf (Fig. 2C), the shallowest SMI depth observed or inferred in the CR-BR area.

The inference that linear sulfate gradients indicate a focused sink for pore-water sulfate over the breadth of the Blake Ridge, as well as the occurrence of large ^{13}C depletions in interstitial ΣCO_2 and methane (Borowski et al., 1996, 1997), prompted us to sample Leg 164 sediments in an unusually detailed manner. Our objective was to gather additional supportive evidence documenting the occurrence of AMO, and to quantify its role in sulfate depletion in methane-rich, gas-hydrate settings.

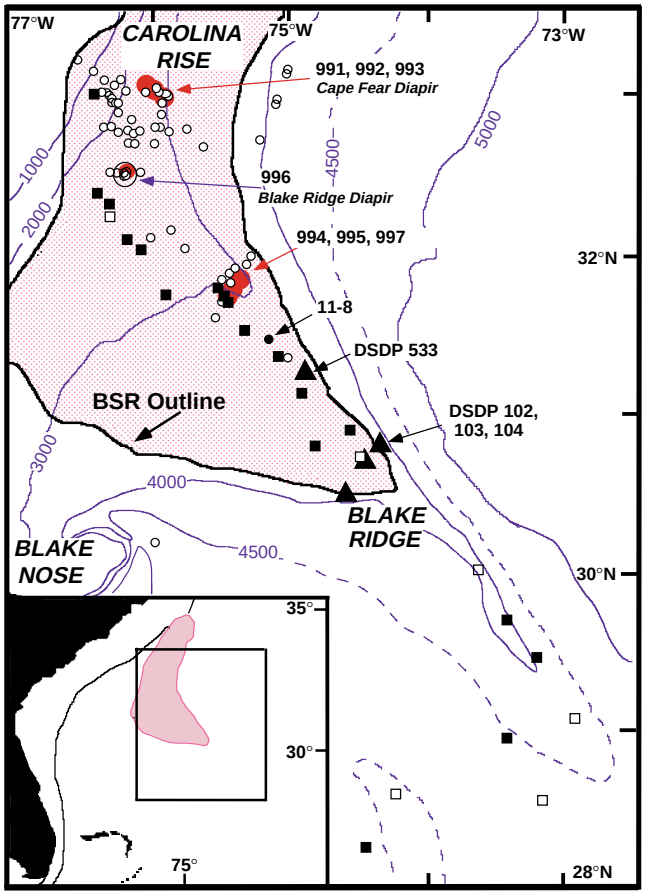

Figure 1. Map showing the location of ODP Leg 164 sites (large, solid circles), DSDP sites (solid triangles), and piston cores (small circles and squares; Borowski et al., 1997). Bathymetric contours are in meters after Uchupi (1968). The outline of bottom-simulating reflectors (BSRs; shaded) is based on the mapping of Dillon and Paull (1983).

METHODS

Pore-water data from the Blake Ridge (Fig. 1) were gathered from sediments collected by both ODP operations on Leg 164 and piston coring.

Sediment Sampling and Geochemical Measurements

Procedures for collecting and processing piston core sediments and their pore waters are described in Borowski (1998). Sediments collected from ODP cores were sampled and processed using standard ODP methods, except that pore-water samples were taken more frequently at every ~1.5 m (1 sample per section, or 6 samples per core) (e.g., Fig. 3). Pore waters were extracted from sediments using a hydraulic sediment press (Manheim, 1966) and collected in airtight syringes (Manheim and Sayles, 1974). Sulfate concentration was determined by ion chromatography, and alkalinity was measured by titration (Gieskes et al., 1991). Total carbon dioxide (ΣCO_2) was separated and measured onshore using cyrogenic and manometric techniques (Craig, 1953) from pore-water aliquots stored immediately after squeezing in flame-sealed, airtight ampoules. Methane concentrations within piston core and Site 994 sediments were measured on shipboard using headspace methods (Martens and Klump, 1980; Kvenvolden and McDonald, 1985; Borowski et al., 1997) and normalized to pore space volume (Paull, Matsumoto, Wallace, et al., 1996). Methane concentrations from Site 995 pore waters were measured from subcores transported to an onshore laboratory, and normalized to pore space volume (Hoehler et al., Chap. 8, this volume).

ΣCO_2 was separated and purified using cryogenic techniques (e.g., Craig, 1953). Carbon-isotopic–composition measurements of ΣCO_2 are reported relative to the Peedee belemnite (PDB) standard, and were made using a Delta E mass spectrometer at North Carolina State University (NCSU). The cumulative (vacuum line and mass spectrometer) accuracy and precision of isotopic measurements are ±0.2‰ and ±0.06‰ (Neal Blair, pers. comm., 1996).

Sulfur isotopic measurements of interstitial sulfate were made at Geochron Laboratories (Cambridge, MA). Sulfate within pore waters was precipitated as barium sulfate, thermally decomposed to SO_3, and reduced to SO_2 gas for isotopic measurement (Holt and Engelkemeir, 1970). Measurements were made using a VG Micromass mass spectrometer (Model 903), and are reported relative to the Canyon Diablo Troilite (CDT) standard. Measurement precision is ±0.1‰ and cumulative accuracy is ±0.3‰ (Marshall Otter, pers. comm., 1997).

Diagenetic Model

Variations in the concentration of interstitial constituents relative to time and depth can be described by equations relating the mass-

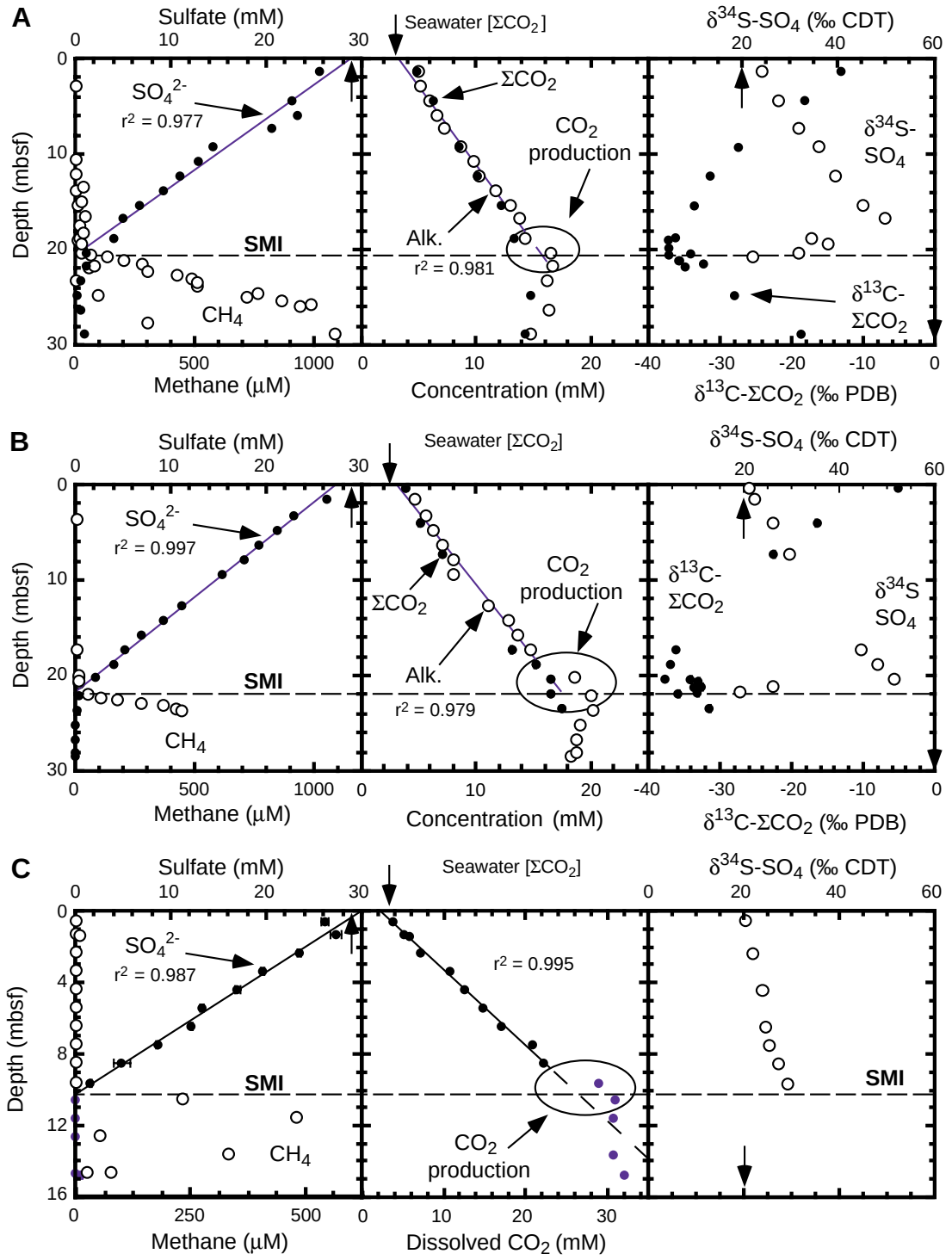

Figure 2. Pore-water concentration profiles for sulfate (SO_4^{2-}) and methane (CH_4); total dissolved carbon dioxide (ΣCO_2) and alkalinity (Alk.); and isotopic composition profiles of $\delta^{13}C_{\Sigma CO_2}$ and $\delta^{34}S_{SO_4}$ for (**A**) Site 994, (**B**) Site 995, and (**C**) piston core (PC) 11–8. Concentration is expressed in millimolar (mM) units for sulfate, ΣCO_2, and alkalinity; methane concentration is expressed in micromolar (μM) units. Measurement uncertainties are shown with error bars, but are generally smaller than symbol size. Carbon isotopic composition is relative to the Peedee belemnite (PDB) standard; sulfur isotopic compositions are relative to Canyon Diablo Troilite (CDT). Representative seawater values for concentration and isotopic composition are shown with solid arrows pointing to the x-axes. The sulfate-methane interface (SMI) is shown by the horizontal dashed lines. Sulfate gradients are linear (note correlation coefficients, r^2, from least-square regression) within >95% probability (r test; Young, 1962).

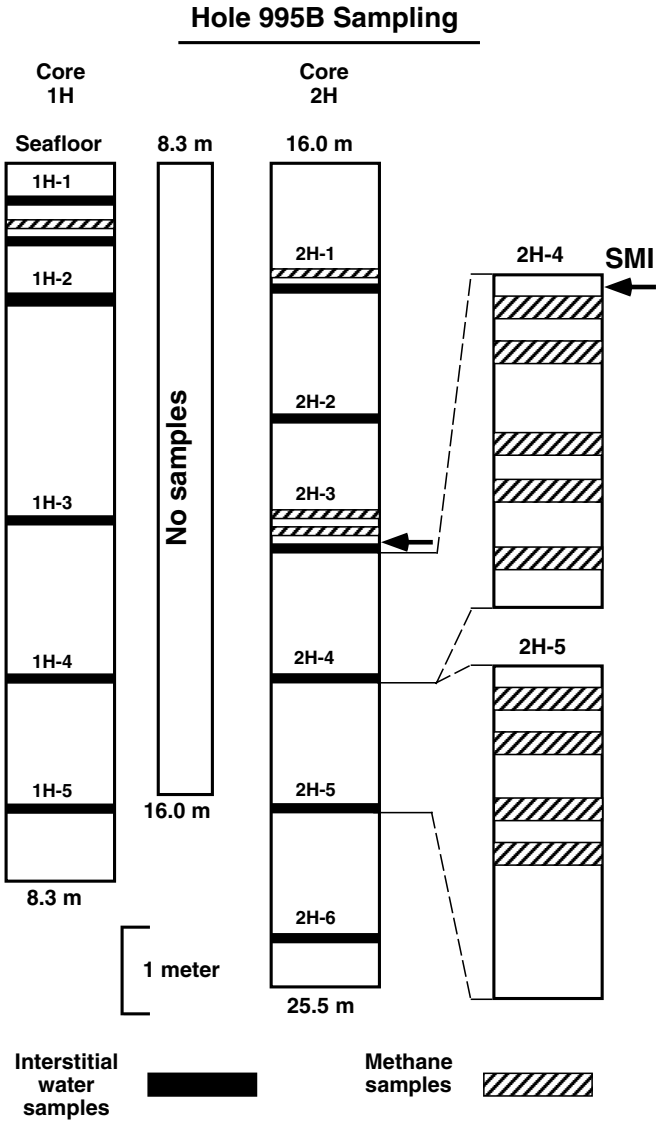

Figure 3. Schematic diagram showing the high-resolution sampling of sediments in Hole 995B. Cores 164-995B-1H and 2H sampled the sulfate-reduction and uppermost methanogenic zones. Core depths in meters (m) are cumulative; note that sediments from 8.3 to 16 m were not sampled. Also note that two sections of Core 164-995B-2H (Sections 2H-4 and 5) were sampled further to measure methane concentrations (Table 3; Hoehler et al., Chap. 8, this volume). The sulfate-methane interface (SMI) at Site 995 is at 20.5 meters below seafloor (mbsf). Samples 4.5 m above and 5 m below the SMI were taken in the same core (Core 164-995B-2H), so that the samples accurately record depths (with concentration and isotopic data) relative to the SMI.

transport processes of diffusion, advection (burial and compaction) to consumption and production reactions (e.g., Berner, 1980). The general diagenetic equation used here is

$$\frac{\partial C}{\partial t} = \phi^2 D_o \frac{\partial^2 C}{\partial x^2} + \left(3\phi D_o \frac{\partial \phi}{\partial x} - \frac{\omega_\infty \phi_\infty}{\phi_x}\right)\frac{\partial C}{\partial x} + R_x = 0, \qquad (3)$$

where C is concentration, t is time, ϕ is porosity, D_o is the free-solution diffusion coefficient, x is depth below the sediment-water interface, ω is sedimentation or burial rate, and R is reaction rate (Berner, 1964, 1977). The subscript (∞) refers to the depth where $\partial\phi/\partial x$ approaches zero. This form of the diagenetic equation was initially applied to anoxic, methane-oxidizing sediments by Murray et al. (1978).

The model explicitly assumes that: (1) steady state conditions occur (i.e., $\partial C/\partial t = 0$); (2) vertical concentration gradients are much greater in magnitude than horizontal gradients; (3) sediment burial, compaction, and molecular diffusion are the only mass-transport processes (no fluid advection, bioirrigation, or gas ebullition occurs); (4) the free-solution diffusion coefficient and sediment density are constant with depth; and (5) the diffusion coefficient within sediment (D_s) is related to free-solution diffusion coefficient by the expression, $D_s = \phi^2 D_o$ (Ullman and Aller, 1982).

An inverse, numerical model was used to predict reaction rates and their depth distribution using Equation 3 by solving for R_x for data collected at Site 995 (for model parameters see Table 1). Cubic spline functions were used to fit methane concentration data providing the necessary gradient information used to calculate the first and second derivative terms of Equation 3. Cubic splines are particularly good for fitting purposes because they: (1) have no inherent functional form (e.g., like exponential or polynomial functions); (2) have continuous first and second derivatives; and (3) can be modified to accept measurement uncertainties (Ahlberg et al., 1967; Alperin, 1988; Alperin et al., 1988). Porosity data (Paull, Matsumoto, Wallace, et al., 1996) were fit using an exponential function that provided ϕ_x and ϕ_∞. The free-solution coefficient (D_o) used for methane was 7.9×10^{-6} cm^2 s^{-1} (3°C; calculated from empirical data given by Li and Gregory, 1974; Lerman, 1979), based on a sediment temperature of ~4°C (Ruppel, 1997). The sedimentation rate was assumed to be constant at 0.0057 cm y^{-1} (5.7 cm ky^{-1}), based on the last appearance of *Pseudoemiliania lacunosa* (Paull, Matsumoto, Wallace, et al., 1996), which occurred at 0.46 Ma (Thierstein et al., 1977).

RESULTS

Sulfate Gradients

Sulfate gradients at Sites 994, 995, and 997 are linear through most of the sulfate reduction zone (Site 994, Fig. 2A; Site 995, Fig. 2B; Site 997, not shown, see Paull, Matsumoto, Wallace et al., 1996; Table 2). Sulfate gradients calculated by least-square linear regression are 1.41, 1.30, and 1.23 mM m^{-1} respectively for the three sites; the sulfate-methane interface lies at 20.5, 21.0, and 22.7 mbsf. The sulfate gradient in piston core (PC) 11–8 is 2.88 mM m^{-1} with a SMI depth of 10.3 mbsf (Fig. 2C).

Table 1. Model conditions and parameters for the finite difference, diffusion-advection-reaction model used to estimate methane reaction rates.

Parameter	Value	Source
ϕ	$0.266 \times \exp(-0.0000235 \times x) + 0.459$	Exponential fit to measured porosity data (Paull, Matsumoto, Wallace, et al., 1996)
ϕ_∞	0.459	Fit to porosity data
ω	5.7 cm ky^{-1}	Last appearance, *Pseudoemiliania lacunosa* (Paull, Matsumoto, Wallace, et al., 1996)
$D_o - CH_4$	7.9×10^{-6} cm^2 s^{-1}	3°C (Li and Gregory, 1974; Lerman, 1979)

Note: x = sediment depth (cm).

Table 2. Interstitial water data for samples shallower than 60 mbsf, Sites 994, 995, and 997, and piston core 11–8.

Core, section, interval (cm)	Depth (mbsf)	Chloride (mM)	Alkalinity (mM)	ΣCO_2 (mM)	Uncertainty ΣCO_2 (mM)	Sulfate (mM)	$\delta^{13}C$-ΣCO_2 (‰ PDB)	Uncertainty $\delta^{13}C$-ΣCO_2 (‰ PDB)	$\delta^{34}S$-SO_4 (‰ CDT)
164-994A-									
1H-1, 140-150	1.40	555	5.0	4.93	0.00	25.6	–13.04	0.06	23.9
1H-2, 140-150	2.90	557	5.2	—	—	23.9	—	—	—
1H-3, 140-150	4.40	557	6.0	6.29	0.05	22.7	–18.25	0.04	27.2
1H-4, 140-150	5.90	558	6.5	—	—	23.2	—	—	—
1H-5, 140-150	7.40	557	7.2	—	—	20.6	—	—	31.4
2H-1, 140-150	9.30	560	8.7	8.48	0.00	14.4	–27.46	0.03	35.7
2H-2, 140-150	10.80	559	9.8	—	—	12.9	—	—	—
2H-3, 140-150	12.30	560	10.3	10.10	0.00	11.1	–31.39	0.03	39.2
2H-4, 140-150	13.80	559	11.7	—	—	9.2	—	—	—
2H-5, 140-150	15.30	556	13.0	12.16	0.04	6.8	–33.63	0.04	45.0
2H-6, 140-150	16.80	558	13.8	—	—	5.1	—	—	49.6
3H-1, 140-150	18.80	558	14.3	13.24	0.07	4.1	–36.09	0.03	34.2
3H-2, 10-25	19.00	—	—	13.90	0.04	—	–37.17	0.04	—
3H-2, 45-60	19.35	—	—	13.47	0.00	—	–37.28	0.04	37.7
3H-2, 80-95	19.70	—	—	14.15	0.04	—	–37.23	0.04	—
3H-2, 115-130	20.05	—	—	14.11	0.07	—	–37.28	0.06	—
3H-2, 140-150	20.30	558	16.5	16.03	0.04	1.2	–37.25	0.06	31.7
3H-3, 10-25	20.50	—	—	15.10	0.00	—	–34.16	0.05	—
3H-3, 45-60	20.85	—	—	15.14	0.08	—	–35.61	0.03	21.9
3H-3, 80-95	21.20	—	—	14.98	0.00	—	–35.67	0.06	—
3H-3, 115-130	21.55	—	—	14.76	0.07	—	–32.20	0.04	—
3H-3, 140-150	21.80	559	16.6	15.24	0.00	1.3	–35.00	0.04	—
3H-4, 140-150	23.30	558	16.2	—	—	0.7	—	—	—
3H-5, 140-150	24.80	558	—	14.80	0.04	0.2	–28.06	0.08	—
3H-6, 140-150	26.30	558	16.4	—	—	0.6	—	—	—
4H-2, 140-150	28.89	555	14.8	14.20	0.04	1.0	–18.80	0.06	—
4H-3, 140-150	30.39	557	15.3	—	—	1.4	—	—	—
4H-4, 140-150	31.89	555	17.0	13.71	0.08	0.2	–17.65	0.05	—
4H-6, 140-150	34.89	552	16.6	15.47	0.04	1.0	–11.65	0.05	—
164-994C-									
5H-5, 145-150	40.35	551	19.0	18.41	0.08	0.0	–4.35	0.03	—
6H-4, 145-150	48.05	552	23.8	21.46	0.14	0.3	0.51	0.06	—
7H-4, 145-150	57.85	549	26.3	24.12	0.27	0.0	2.59	0.05	—
164-995A-									
5H-5, 145-150	37.65	553	20.2	17.76	0.14	0.0	–9.92	0.03	—
6H-5, 145-150	47.10	546	23.0	21.13	0.00	0.0	–1.74	0.05	—
164-995B-									
1H-1, 38-48	0.38	557	4.0	3.88	0.02	—	–5.07	0.05	21.2
1H-1, 85-95	0.85	558	4.0	—	—	—	—	—	—
1H-2, 0-15	1.50	557	5.9	—	—	27.0	—	—	22.5
1H-3, 66-76	3.66	—	—	—	—	—	—	—	—
1H-3, 108-118	4.08	558	6.0	5.10	0.05	23.6	–16.49	0.05	26.2
1H-4, 140-150	5.90	558	—	—	—	21.7	—	—	—
1H-5, 140-150	7.40	562	7.1	7.04	0.05	19.9	–22.47	0.04	29.7
2H-1, 122-132	17.22	—	—	—	—	—	—	—	—
2H-1, 140-150	17.40	560	15.0	13.09	0.04	6.0	–36.08	0.05	44.5
2H-2, 140-150	18.90	558	18.4	15.15	0.04	3.0	–36.96	0.03	48.1
2H-3, 100-110	20.00	—	—	—	—	—	—	—	—
2H-3, 120-130	20.20	—	—	—	—	—	—	—	—
2H-3, 140-150	20.40	559	19.8	16.49	0.01	1.6	–37.70	0.04	51.6
2H-4, 10-20	20.60	—	—	11.39	0.04	—	–33.92	0.04	—
2H-4, 30-40	20.80	—	—	10.74	0.06	—	–33.08	0.04	—
2H-4, 72-82	21.22	—	—	10.92	0.03	—	–33.28	0.05	26.2
2H-4, 92-102	21.42	—	—	10.86	0.03	—	–32.83	0.06	—
2H-4, 122-132	21.72	—	—	11.55	0.00	—	–32.99	0.03	19.2
2H-4, 140-150	21.90	559	20.4	16.49	0.04	0.0	–35.78	0.05	—
2H-5, 140-150	23.40	558	20.1	17.50	0.04	0.0	–31.50	0.09	—
2H-6, 140-150	24.90	557	19.4	—	—	0.5	—	—	—
164-997A-									
3H-5, 140-150	19.80	559	16.7	15.36	0.00	3.2	–30.82	0.06	—
3H-6, 140-150	21.30	561	17.8	15.59	0.00	1.5	–31.16	0.03	—
4H-1, 140-150	23.30	559	16.6	16.51	0.00	0.2	–25.98	0.05	—
6H-2, 140-150	43.80	545	24.3	23.26	0.00	0.2	–1.72	0.03	—
Piston Core 11-8									
54-60	0.57	542	—	3.8	—	26.1	—	—	20.2
60-70	0.65	—	—	—	—	—	—	—	—
133-139	1.36	543	—	5.2	—	27.3	—	—	—
233-239	2.36	523	—	7.2	—	23.4	—	—	21.8
239-249	2.44	—	—	—	—	—	—	—	—
340-346	3.43	530	—	10.8	—	19.7	—	—	—
440-446	4.43	523	—	12.6	—	17.0	—	—	23.9
540-546	5.45	551	—	14.8	—	13.3	—	—	—
648-654	6.51	534	—	17.0	—	12.2	—	—	24.6
748-754	7.51	534	—	20.8	—	8.6	—	—	25.5
848-854	8.51	549	—	22.2	—	4.9	—	—	27.4
956-962	9.59	557	—	29.0	—	2.1	—	—	29.1
1052-1062	10.55	557	—	30.9	—	0.0	—	—	—
1156-1162	11.59	557	—	30.7	—	0.0	—	—	—
1262-1268	12.65	556	—	—	—	0.0	—	—	—
1362-1368	13.65	—	—	30.8	—	0.0	—	—	—
1462-1468	14.65	543	—	—	—	0.0	—	—	—
1475-1490	14.82	546	—	32.0	—	0.6	—	—	—

Notes: Complete concentration data for Sites 994, 995, and 997 in Paull, Matsumoto, Wallace, et al., (1996). mM = millimoles per liter or millimolar. PDB = Peedee belemnite carbon standard. CDT = Canyon Diablo Troilite sulfur standard. — = not measured.

Methane

Methane concentrations (Table 3) are low through the sulfate reduction zone and then increase rapidly once low (<1 mM) pore-water sulfate concentrations occur (Fig. 2). These data are consistent with the placement of the sulfate-methane interfaces as shown at sites 994, 995, and PC 11–8. Methane concentration data from sites 994 and PC 11–8 are much noisier relative to that of Site 995 because of the crude headspace methods used. The methane data from Site 995 shown in Fig. 2B were obtained from measurements of methane concentration in two subcores, and these duplicate measurements deviate by <5% (Hoehler et al., Chap. 8, this volume).

Interstitial ΣCO_2 and Alkalinity

The ΣCO_2 concentrations increase monotonically as sulfate concentrations decrease (Table 2; Fig. 2). Within the sulfate reduction zone of PC 11–8, ΣCO_2 concentrations are generally linear, but concave-down curvature occurs in the profiles near the sulfate-methane interface. The ΣCO_2 concentrations show little variation immediately below the interface.

The ΣCO_2 concentration data for ODP Sites 994 and 995 are stratigraphically sparse near the sulfate-methane interface (Table 2), so we have also included alkalinity values. Because ΣCO_2 is the predominant control on alkalinity in this system (Fig. 2), the shape of alkalinity profiles mimics ΣCO_2 profiles, with alkalinity also increasing with increasing sulfate consumption downcore. The values are linear in the upper sulfate reduction zone, but alkalinity shows an inflection point near the SMI, where alkalinity is higher than expected based on linear extrapolation from above. Alkalinity values show little variation for about 10 m below the interface, but begin to increase below 30 mbsf (Paull, Matsumoto, Wallace et al., 1996).

$\delta^{13}C$-ΣCO_2

The carbon isotopic composition of dissolved CO_2 of the overlying seawater is near 0 per mil (‰, PDB), but decreases rapidly within interstitial waters of the sulfate reduction zone (Sites 994 and 995, Fig. 2B, C; Table 2). Maximum enrichments of light carbon (^{12}C) occur at the sulfate-methane interface, where $\delta^{13}C_{\Sigma CO_2}$ values are –37.3‰ and –37.7‰, respectively for sites 994 and 995. Further downcore, light carbon composes less of the ΣCO_2 pool. No $\delta^{13}C_{\Sigma CO_2}$ values are available for PC 11–8. At Site 995, $\delta^{13}C$ values more depleted in ^{13}C than –30‰ lie between 13 and 24 mbsf.

$\delta^{34}S$-SO_4

The sulfur isotopic composition of interstitial sulfate changes progressively downcore as sulfate is depleted (Table 2; Fig. 2). Sulfur in modern seawater sulfate has a $\delta^{34}S$ value of +20.0‰ ± 0.1‰, CDT (Rees et al., 1978), and each site shows that interstitial sulfate becomes progressively enriched in heavy sulfur (^{34}S) with increasing depth into the sulfate reduction zone. The fractionation observed in sulfate of PC 11–8 is significantly less than that at Sites 994 and 995, with the respective maximum $\delta^{34}S$ values of +29.1‰, +49.6‰, and +51.6‰.

CALCULATIONS AND MODEL RESULTS

Sulfate Flux

The flux of sulfate into the sediment from overlying seawater can be approximated from linear sulfate gradients using Fick's First Law:

$$J = D_0\phi^3\frac{\partial C}{\partial x}, \quad (4)$$

Table 3. Methane concentration data for Holes 994A and 995B, and for piston core 11-8.

Core, section, interval (cm)	Depth (mbsf)	Methane (µM)
164-994A-*		
1H-1, 140-150	1.40	—
1H-2, 140-150	2.90	1
1H-3, 140-150	4.40	—
1H-4, 140-150	5.90	—
1H-5, 140-150	7.40	—
2H-1, 140-150	9.30	—
2H-2, 115-130	10.55	2
2H-2, 140-150	10.80	—
2H-3, 115-130	12.05	2
2H-3, 140-150	12.30	—
2H-4, 115-130	13.55	18
2H-4, 140-150	13.80	1
2H-5, 115-130	15.05	15
2H-5, 140-150	15.30	7
2H-6, 115-130	16.55	22
2H-6, 140-150	16.80	—
3H-1, 10-25	17.50	11
3H-1, 85-110	18.25	19
3H-1, 140-150	18.80	11
3H-2, 10-25	19.00	5
3H-2, 45-60	19.35	12
3H-2, 80-95	19.70	—
3H-2, 115-130	20.05	12
3H-2, 140-150	20.30	12
3H-3, 10-25	20.50	38
3H-3, 45-60	20.85	80
3H-3, 80-95	21.20	124
3H-3, 115-130	21.55	170
3H-3, 140-150	21.80	53
3H-4, 10-25	22.00	33
3H-4, 45-60	22.35	185
3H-4, 80-95	22.70	261
3H-4, 115-130	23.05	298
3H-4, 140-150	23.30	1
3H-5, 10-25	23.50	314
3H-5, 45-60	23.85	311
3H-5, 80-95	24.20	849
3H-5, 115-130	24.55	469
3H-5, 140-150	24.80	57
3H-6, 10-25	25.00	439
3H-6, 45-60	25.35	532
3H-6, 80-95	25.70	608
3H-6, 115-130	26.05	580
3H-6, 140-150	26.30	—
3H-7, 140-150	27.60	806
4H-2, 10-25	27.60	184
4H-2, 140-150	28.89	668
164-995B-†		
1H-3, 66-76	3.66	9
2H-1, 122-132	17.22	6
2H-3, 100-110	20.00	16
2H-3, 120-130	20.20	17
2H-4, 10-20	20.60	18
2H-4, 30-40	20.80	18
2H-4, 72-82	21.22	54
2H-4, 92-102	21.42	104
2H-4, 122-132	21.72	177
2H-5, 10-20	22.10	274
2H-5, 30-40	22.30	367
2H-5, 60-70	22.60	421
2H-5, 80-90	22.80	442
Piston core 11-8‡		
54-60	0.57	1
60-70	0.65	—
133-139	1.36	1
233-239	2.36	>0
340-346	3.43	1
440-446	4.43	>0
540-546	5.45	>0
648-654	6.51	1
748-754	7.51	>0
848-854	8.51	>0
956-962	9.59	1
1052-1062	10.55	185
1156-1162	11.59	386
1262-1268	12.65	41
1362-1368	13.65	267
1462-1468	14.65	19
1475-1490	14.82	61

Notes: No methane gas hydrates are present at these depths. µM = micromoles per liter or micromolar. * = Paull, Matsumoto, Wallace, et al. (1996; shipboard determinations). — = not measured. † = average values from two samples (from subsamples measured onshore); Hoehler et al. (Chap. 8, this volume). ‡ = Borowski (1998; shipboard determinations).

where J is the flux, D_o is free-solution diffusion coefficient, ϕ is porosity, and $\partial C/\partial x$ is the concentration gradient (e.g., Lerman, 1979). Given a mean sediment porosity of 70% for the sulfate reduction zone (Paull, Matsumoto, Wallace, et al., 1996), sediment temperatures of ~4°C (Ruppell, 1997), and a sulfate diffusion coefficient of 5.8×10^{-6} cm s^{-1} (5°C, Li and Gregory, 1974), the sulfate gradients from Sites 994, 995, and PC 11–8 predict sulfate fluxes of (8.8, 8.2, and 18) $\times 10^{-4}$ mmol cm^{-2} yr^{-1}, respectively.

Mixing Model Results

An established approach of assessing the importance of AMO is to algebraically account for the carbon isotopic contributions of each component comprising the ΣCO_2 pool (Blair and Aller, 1995). The ΣCO_2 sources at the sulfate-methane interface include that from overlying seawater trapped within sediments during burial (sw), that derived from sedimentary organic matter during remineralization (om), and that produced by anaerobic methane oxidation (amo). In a closed system, the carbon isotopic composition of the pool at the SMI is related to its components by:

$$\delta^{13}C_{\text{total pool}} = (X_{sw})(\delta^{13}C_{sw}) + (X_{om})(\delta^{13}C_{om}) + (X_{amo})(\delta^{13}C_{amo}), \quad (5)$$

where X is the constituent's fraction of the total ΣCO_2 pool, $\delta^{13}C$ is the carbon isotopic composition, and the subscripts sw, om, and amo refer to CO_2 donated from the sources listed above. For Site 995, the value of X_{sw} is fixed at 0.139 (seawater ΣCO_2 concentration divided by ΣCO_2 concentration at the SMI, or 2.3 mM/ 16.5 mM) with $\delta^{13}C_{sw}$ equal to 0‰. The isotopic value of sedimentary organic matter at the Blake Ridge averages –21‰ ± 3‰ PDB (N= 120; Brooks et al., 1983; Olsen, 1997), and this value is used for $\delta^{13}C_{om}$. The isotopic composition of methane at the interface is –101‰ PDB (Hoehler et al., Chap. 8, this volume), and this value is used for $\delta^{13}C_{amo}$ (assuming no fractionation during AMO). The proportions of C_{om} and C_{amo} composing the remaining fraction of the ΣCO_2 pool (1.0 – 0.139 = 0.861) are varied to produce the mixing line in Figure 4.

The mixing model estimates that ~24% of the carbon within the CO_2 pool at the sulfate-methane interface is derived from methane (Fig. 4). This is only a crude estimate because the system is open (i.e., CO_2 diffusion occurs), because carbonate mineral precipitation occurs (Rodriguez et al., Chap. 30, this volume), and because carbon fractionation occurs during AMO.

Diagenetic Model Results

Modeling of methane concentrations provides an independent estimate of the amount of sulfate consumed by AMO. Although in situ methane concentrations of deep-water sediments are difficult to measure accurately (Paull et al., unpubl. data), methane concentrations less than the methane bubble saturation at surface temperature and pressure should reflect in situ concentrations because loss of methane through outgassing is unlikely. Hence, the methane concentration data (Table 3) are apparently suitable for modeling.

The method assumes steady state conditions so that the distribution and magnitude of reaction rates can be solved for by fitting observed concentration data and solving the diagenetic equation (Eq. 3) for R_x using numerical methods. A cubic spline fit to the methane concentrations measured in Site 995 sediments (Hoehler et al., Chap. 8, this volume) approximates these data well (Fig. 5A). The measured methane profile has inflections (see arrows Fig. 5A), accurately reflected in the cubic spline fit, that produce variations in the first and second derivatives. The model results identify the depths where methane consumption and methane production are expected, and indicates the magnitude of the reaction rates as a function of depth (Fig. 5B). Model results also show that methane consumption occurs over a 2-m interval (~20.5–22.5 mbsf), and that methane production occurs immediately below (Fig. 5B). The modeled AMO reaction rates show peak values approaching 5 µM yr^{-1} (0.005 µmol cm^{-3} yr^{-1}) just below 21 mbsf.

The integrated methane flux corresponds to the area under the first derivative of the cubic spline fit (not shown). The model predicts a total upward methane flux of 2.9×10^{-4} mmol cm^{-2} yr^{-1}. At Site 995, the corresponding total sulfate flux, calculated using Fick's First Law, is 8.2×10^{-4} mmol cm^{-2} yr^{-1}. Thus, approximately 35% of the total sulfate flux into the sediment is used to consume upwardly diffusing methane.

Model results from fitting the methane concentration values agree well with concentration and isotopic data. As expected, the slight inflection in the concentration trend within the methanogenic zone (Fig. 5A) causes the model to predict a shift from methane production to methane consumption, and the large inflection in methane concentration at the SMI coincides with peak methane oxidation rates. Furthermore, minimum $\delta^{13}C_{\Sigma CO_2}$ values are coincident with peak methane oxidation rates.

DISCUSSION

Evidence for Anaerobic Methane Oxidation

Together with a strongly concave-up methane profile (Martens and Berner, 1974), several additional lines of evidence indicate that sulfate and methane co-consumption occurs at the sulfate-methane interface: (1) ΣCO_2 and alkalinity profiles indicate localized CO_2 production there; (2) $\delta^{13}C_{\Sigma CO_2}$ values are extremely depleted in ^{13}C, and are lowest within the logical depth-zone for AMO; and (3) sulfate gradients are linear throughout the sulfate-reduction zone.

The magnitude and position of isotopic values of ΣCO_2 provide the most compelling evidence for AMO (e.g., Reeburgh, 1980). The $\delta^{13}C_{\Sigma CO_2}$ values more negative than –30‰ PDB most likely indicate derivation from methane because the isotopic carbon composition of marine phytoplankton is generally heavier than –30‰ (Deines, 1980). In addition, $\delta^{13}C_{\Sigma CO_2}$ values reach their lightest (–37.7‰) at the SMI, where CO_2 production is indicated by deviation from linearity in the ΣCO_2 and alkalinity profiles (Fig. 2). This local increase in ΣCO_2 is consistent with production of ^{12}C-rich CO_2 through sulfate and methane co-consumption, and the diffusion of light CO_2 away from the SMI. Near invariant alkalinity and ΣCO_2 concentrations some meters below the SMI are consistent with a net sink for interstitial CO_2 in the uppermost methanogenic zone due to carbonate mineral authigenesis (Rodriguez et al., 1997, and Chap. 30, this volume).

Assuming steady state conditions, linear sulfate gradients within the sulfate-reduction zone are circumstantial evidence for focused consumption of sulfate at the sulfate-methane interface by AMO. Linear profiles imply sulfate diffusion through the sulfate-reduction zone and consumption at the interface where sulfate and methane co-occur (Borowski et al., 1996).

Microbial consumption of sulfate to form interstitial dissolved sulfide ($\Sigma HS^-_{\text{dissolved}} = S^{2-} + HS^- + H_2S$) preferentially uses light (^{32}S) sulfur by both sulfate reduction of SOM (Eq. 1) and AMO (Eq. 2). These fractionations create a dissolved sulfide pool depleted in heavy sulfur (^{34}S; typically negative $\delta^{34}S$ values), and create progressive enrichments of ^{34}S in the residual sulfate pool ($\delta^{34}S$ values more positive than +20‰) (e.g., Chambers and Trudinger, 1979; Goldhaber and Kaplan, 1974). Although the sulfur isotopic composition of interstitial sulfate indicates microbial fractionation at all sites (11–8, 994, 995; Fig. 2), either or both sulfate-depleting mechanisms could qualitatively account for the observed $\delta^{34}C_{SO_4}$ profiles.

Intensity of AMO

The intensity of anaerobic methane oxidation operating at the sulfate-methane interface can be gauged by appraising how much methane carbon resides in the ΣCO_2 pool, or by estimating the pro-

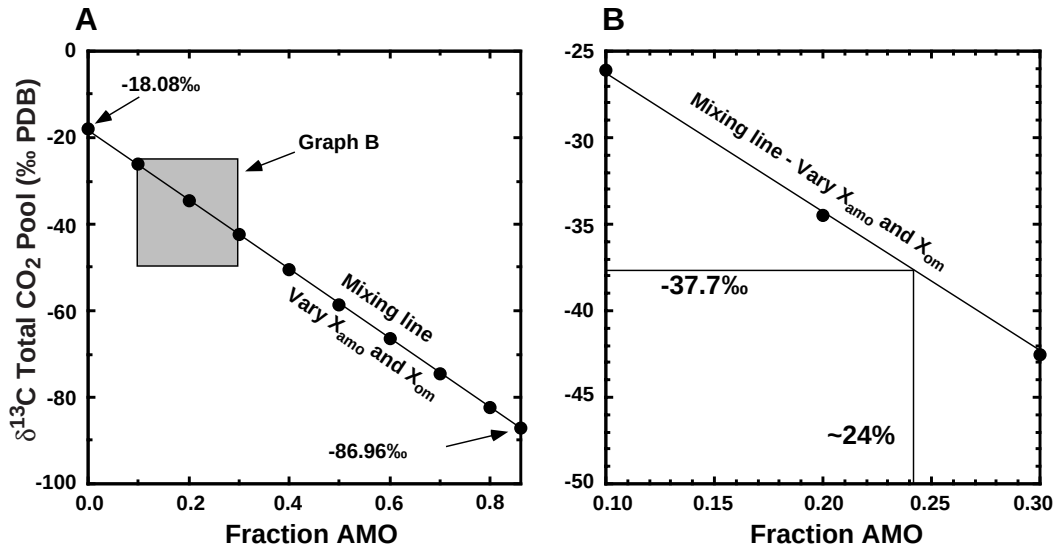

Figure 4. **A.** Diagram showing how varying amounts of carbon derived from methane via anaerobic methane oxidation (Fraction AMO) affect the carbon isotopic composition of the ΣCO_2 pool ($\delta^{13}C_{\Sigma CO_2}$). **B.** An enlargement of the shaded box in A. The measured carbon isotopic composition of the ΣCO_2 pool at the sulfate-methane interface at Site 995 is –37.7‰. Using this value, the model predicts that the ΣCO_2 pool has received ~24% of its carbon from methane, presumably through AMO.

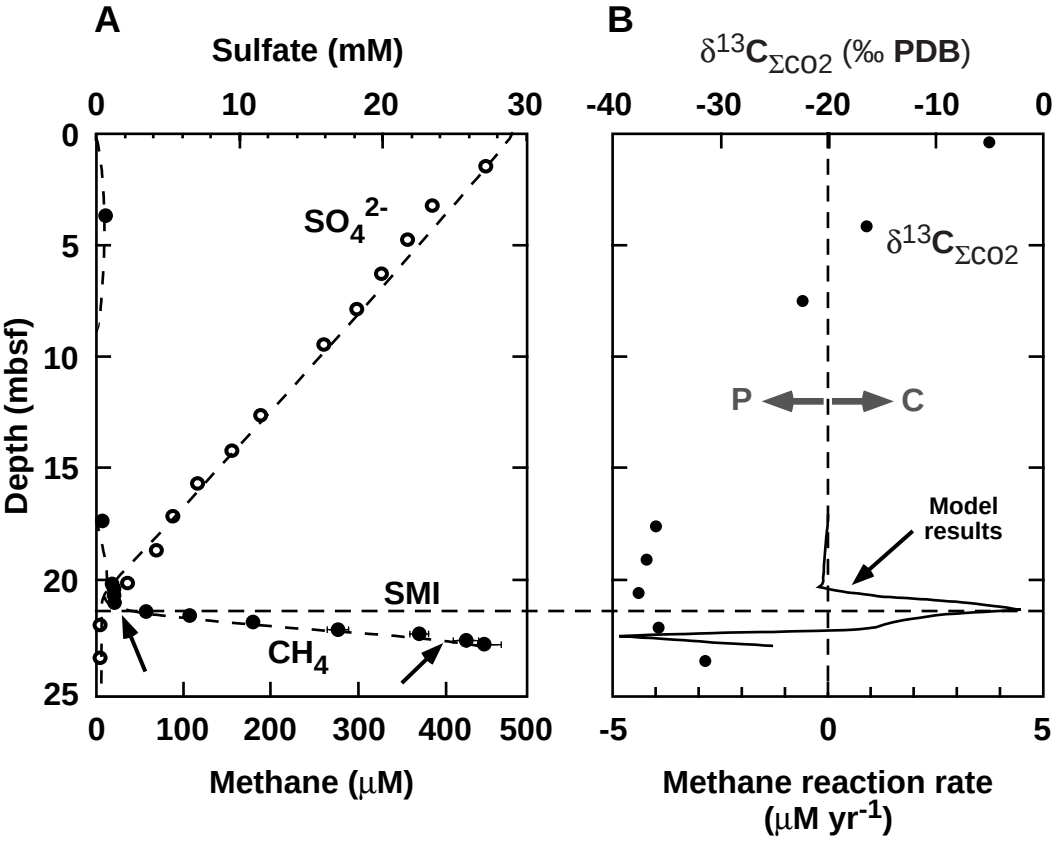

Figure 5. Graphs showing model results for Site 995 data. **A.** Sulfate concentrations (Paull, Matsumoto, Wallace, et al., 1996) and methane concentrations (Hoehler et al., Chap. 8, this volume) measured at Site 995. A cubic spline function was used to fit the methane concentration profile. Inflections in the methane concentration trend are highlighted with arrows. The dashed line associated with sulfate concentrations is not a linear regression fit to the data like that in Figure 2B, but was calculated by the numerical model by increasing methane oxidation rates seen in Figure 2B by approximately three times. **B.** Zones for methane production (P) and consumption (C) predicted by the model, and calculated methane reaction rates (R) are in units of mM yr^{-1} (or mmol cm^{-3} yr^{-1}). $\delta^{13}C$ values of the dissolved CO_2 (ΣCO_2) pool are plotted for comparison.

portion of sulfate that AMO consumes relative to total sulfate flux into the sediments. Thus, we assess the importance of AMO at Site 995 using two independent methods: (1) a simple mixing model that considers the sources of ΣCO_2 carbon (Eq. 5); and (2) a diagenetic model that utilizes the interstitial methane concentration profile to estimate methane consumption at the SMI (Eq. 3).

Mixing Model

The ΣCO_2 mixing model suggests that 24% of the carbon within the ΣCO_2 pool has come from methane, but there are biases that affect this calculation. The largest potential bias is the diffusion of ^{12}C-rich CO_2 away from the sulfate-methane interface as suggested by the $\delta^{13}C_{\Sigma CO_2}$ profiles (Fig. 2). Such diffusive processes would act to lower the quantity of light carbon within the ΣCO_2 pool and to lower the estimate of methane carbon.

Alternatively, carbonate mineral formation and the assumption of no carbon fractionation during AMO result in an overestimation of methane carbon within the CO_2 pool. Fractionation during AMO allows entry of more ^{12}C into the CO_2 pool, but from a smaller proportion of methane. Thus, the model calculation overestimates the quantity of methane carbon in the ΣCO_2 pool, however, an isotopic fractionation factor for AMO of 1.002–1.014 (Whiticar and Faber, 1986; Alperin et al., 1988) changes the calculation by only a few percent.

Carbonate mineral formation occurs within the zone of AMO (Rodriguez et al., Chap. 30, this volume), affecting ΣCO_2 concentration. Large losses of CO_2 only slightly affect the isotopic mass balance by changing the proportion of CO_2 derived from seawater (X_{sw}), and therefore altering the mix of CO_2 carbon derived from organic matter (X_{om}) and methane (X_{amo}). Thus, the major effect of an open system on the model calculation lies not in the change of CO_2 concentration, but in its effect on the isotopic composition of the CO_2 pool. Accordingly, because the carbon fractionation involved in carbonate mineral formation is small (e.g., Emrich et al., 1970; Anderson and Arthur, 1983), the isotopic balance calculation is unaffected by this process.

The above factors interact to slightly vary the results of the mixing model, but the largest bias—diffusion of ^{12}C-rich CO_2—acts to underestimate the contribution of methane carbon to the CO_2 pool. The mixing model is relatively insensitive to ΣCO_2 concentration and the AMO fractionation factor, cumulatively changing the estimate of the fraction of methane carbon to between 19% and 24%. A comprehensive interpretation is that at least one-fifth to one-fourth of the carbon within the CO_2 pool is derived from methane through AMO.

Diagenetic Model

The diagenetic model based on methane concentrations does consider diffusive processes and is unaffected by fractionations inherent in microbially mediated reactions because it contains no isotopic inputs. Thus, it is potentially a better tool in assessing the intensity of AMO. Based on methane concentration values, the model predicts that 35% of the total sulfate flux is consumed by AMO, but this may be an underestimate.

The linear sulfate profile of PC 11–8 (Fig. 2C) was reproduced by a finite difference diagenetic model that consumed 95% of the calculated sulfate flux through AMO (Borowski et al., 1996; Borowski, 1998). Increasing contributions of sulfate depleted by oxidation of SOM (Eq. 1), cause increasing curvature in the model results and increasing deviation from the observed sulfate concentration values. A similar predominant proportion of sulfate depletion due to AMO is necessary to approximate the sulfate data at Site 995 (see fit to sulfate data in Fig. 2A). The conundrum is that the model results based on methane data predict a much smaller proportion of sulfate consumed by AMO than do model results based on sulfate concentrations, although each model is internally consistent.

To adjust model results based on methane data to predict higher amounts of sulfate depletion due to AMO, in situ methane concentrations would have to be significantly higher than measured values. Methane loss may occur through outgassing, diffusion, and consumption by aerobic or anaerobic methane oxidation. However, the coincidence of modeled peak methane oxidation rates with the most ^{13}C-depleted $\delta^{13}C_{\Sigma CO_2}$ values suggest that the measured methane concentrations faithfully reproduce at least relative changes in methane concentration.

To adjust sulfate data to reflect lower amounts of sulfate depletion due to AMO, in situ sulfate concentrations must be lower than measured concentrations, or sulfate must be renewed in situ. There are three known mechanisms that could add additional sulfate: (1) oxidation of interstitial dissolved sulfide during sediment and pore-water processing (e.g., Almgren and Hagstrom, 1974); (2) oxidation of sulfide minerals during processing; or (3) in situ anaerobic oxidation of dissolved sulfide by manganese and/or iron oxide minerals (Sorensen and Jorgensen, 1987; Aller and Rude, 1988; Fossing and Jorgensen, 1990; Elsgaard and Jorgensen, 1992; Schulz et al., 1994).

However, sulfide concentration and sulfur isotopic data show no obvious indication that these processes occur in Blake Ridge sediments:

a. Typical interstitial dissolved sulfide concentrations in Blake Ridge pore waters are usually <10 µM and almost always less than 120 µM (except at methane seep sites, Paull et al., 1995; Borowski, 1998). Thus, only a very small amount of oxidized sulfide could be added to the sulfate pool as an artifact of sampling.
b. Sulfide minerals in the sulfate reduction zone of Sites 994, 995, and 997 have a mean $\delta^{34}S$ value of –38.8‰ ± 5.3‰ (N = 30, Borowski, 1998). Pore-water $\delta^{34}S_{SO_4}$ values consistently show ^{34}S enrichment at all sites (Fig. 2), rather than showing any addition of light sulfur from light sulfide derived from oxidized sulfide minerals. Thus, the data do not indicate that the oxidation of very ^{34}S-depleted sulfide minerals during core handling has occurred.
c. To significantly alter sulfate concentration gradients, sizeable amounts of dissolved sulfide, derived from sulfate consumed by sulfate reduction processes, must be oxidized in situ. Because of the argument in (b), if this process occurs it is masked by sulfur disproportionation reactions (Canfield and Thamdrup, 1994). Although there is ample evidence for anoxic sulfide oxidation elsewhere (see references above), we cannot identify its effects in Blake Ridge sediments. Moreover, we infer that anoxic sulfide oxidation is most likely to occur preferentially within the uppermost portion of anoxic sediments (where iron and manganese oxides are readily available; e.g., Aller and Rude, 1988), not deep within the sulfate-reduction zone.

To summarize, we have confidence in our data, but have not resolved the inconsistencies between the different model results. Either there is some undiscovered defect in the models or model assumptions, or there are unrecognized processes that we cannot adequately account for, nor quantify. Future modeling attempts may resolve the issue, especially by testing how modified diagenetic models predict the magnitude and distribution of $\delta^{13}C_{\Sigma CO_2}$ and $\delta^{13}C_{CH_4}$ values. Even with the inconsistencies between model results using methane versus sulfate data, a conservative interpretation is that 35% of the total sulfate flux is consumed by AMO at Site 995.

Areal Variation

There is evidence for a still larger role for AMO, relative to the results at Site 995, at other sites of the CR-BR area. Fully 40% (17 of 42) of the nondiapir sites over the Carolina Rise and Blake Ridge

have sulfate gradients steeper than those observed at Site 995 (Borowski, 1998). If sulfate consumption through AMO induces linearity in the sulfate profiles, we infer that these sites may have a larger proportion of sulfate depleted via AMO versus sulfate reduction of SOM. For example, Site PC 11-8 (Fig. 2C) shows the largest amount of sulfate depletion recorded at nondiapir sites with a gradient of 2.88 mM m^{-1} (vs. 1.30 mM m^{-1} at Site 995), a SMI depth of 10.3 mbsf (vs. 21 msbf at Site 995), and a predicted sulfate flux of 18×10^{-4} mmol cm^{-2} yr^{-1}, or 2.2 times that of Site 995 (8.2×10^{-4} mmol cm^{-2} yr^{-1}).

Implications

The indication that AMO is such a significant sink for interstitial sulfate in these deep-sea sediments is surprising. Large fractions of sulfate consumed by AMO have been documented elsewhere (Table 4), but only at seep or advective sites (not tabulated; e.g., Suess and Whiticar, 1989; Masuzawa, et al., 1992; Cragg et al., 1995; Paull et al., 1995) in organic-rich coastal marine environments (e.g., Saanich Inlet, see Table 4 for references), or in marine basins that have anoxic water columns such as the Black Sea (Reeburgh et al., 1991) and Cariaco Trench (Reeburgh, 1976). Unlike these anoxic basins, the overlying water of the CR-BR area is oxygenated, implying a different impetus for intensified AMO.

Borowski et al. (1996) suggested that the magnitude of upward methane flux controls the intensity of AMO occurring at the sulfate-methane interface, which in turn influences sulfate concentrations (and perhaps produces linear sulfate gradients). Pore-water data presented here, especially $\delta^{13}C_{\Sigma CO_2}$ data, firmly establish AMO as an important diagenetic process at Site 995. Although independent diagenetic modeling results are inconsistent, or do not fully explain the data, a model using methane concentrations (Site 995) suggests that 35% of the total sulfate flux is consumed by AMO. Such large proportions of AMO must affect sulfate concentration gradients. If such an enlarged role for AMO is indeed fueled by upward methane flux, we infer that similar interstitial chemistries should also occur at other continental rise, methane-rich, gas hydrate–associated settings. Thus, steep (and linear) sulfate gradients may be a geochemical indicator of methane-rich sediments, and may also be an indicator for the presence of gas hydrates in continental rise sediments, given that conditions are suitable for gas hydrate formation.

CONCLUSIONS

1. A unique, high-resolution data set consisting of pore-water concentration and isotopic data was gathered through the sulfate-reduction zone and within the uppermost methanogenic zone of Sites 994, 995, and 997 (ODP Leg 164).

2. Linear sulfate gradients are common within the sediments of the Carolina Rise and Blake Ridge, occurring at widely distributed ODP and piston-core sites.

3. Concave-up methane profiles, linear sulfate gradients, patterns of interstitial dissolved CO_2 concentration, and extremely ^{13}C-depleted $\delta^{13}C_{\Sigma CO_2}$ values consistently suggest that anaerobic methane oxidation is a significant sulfate-consuming process at all three ODP sites.

4. An inverse diagenetic model based on measured interstitial methane concentrations estimates that 35% of the total sulfate flux into the sediments at Site 995 is consumed by anaerobic methane oxidation.

5. Forty percent of the (nondiapir) sites sampled in the CR-BR area (by both piston coring and drilling operations) possess linear sulfate gradients larger than that seen at Site 995, implying that anaerobic methane oxidation may be responsible for even larger proportions of total sulfate depletion at these sites.

6. The wide occurrence of steep (linear) sulfate gradients over the Carolina Rise and Blake Ridge suggests that anaerobic methane oxidation is an important, additional process in consuming interstitial sulfate in these gas hydrate–associated sediments. Methane-rich sediments elsewhere, including those associated with gas hydrates, are expected to display similar chemistries.

REFERENCES

Ahlberg, J., Nilson, E., and Walsh, J., 1967. *The Theory of Splines and Their Applications*: San Diego (Academic Press).

Aller, R.C., and Rude, P.D., 1988. Complete oxidation of solid phase sulfides by manganese and bacteria in anoxic marine sediments. *Geochim. Cosmochim. Acta*, 52:751–765.

Almgren, T., and Hagstrom, I., 1974. The oxidation rate of sulphide in sea water. *Water Res.*, 8:395–400.

Alperin, M.J., 1988. The carbon cycle in an anoxic marine sediment: concentrations, rates, isotope ratios, and diagenetic models [Ph.D. dissert.]. Univ. of Alaska, Fairbanks.

Alperin, M.J., Blair, N.E., Albert, D.B., Hoehler, T.M., and Martens, C.S., 1992. Factors that control the stable carbon isotopic composition of methane produced in an anoxic marine sediment. *Global Biogeochem. Cycles*, 6:271–291.

Alperin, M.J., and Reeburgh, W.S., 1984. Geochemical observations supporting anaerobic methane oxidation. *In* Crawford, R.L., and Hanson, R.S. (Eds.), *Microbial Growth on C-1 Compounds.* Am. Soc. Microbiol., 282–298.

Alperin, M.J., Reeburgh, W.S., and Whiticar, M.J., 1988. Carbon and hydrogen fractionation resulting from anaerobic methane oxidation. *Global Biogeochem. Cycles*, 2:279–288.

Anderson, T.F. and Arthur, M.A., 1983. Stable isotopes of oxygen and carbon and their applications to sedimentologic and paleoenvironmental problems. *In* Arthur, M.A., Anderson, T.F., Kaplan, I.F., Veizer, J., and Land, L.S. (Eds.), *Stable Isotopes in Sedimentary Geology.* SEPM Short Course, 10.

Barnes, R.O., and Goldberg, E.D., 1976. Methane production and consumption in anoxic marine sediments. *Geology*, 4:297–300.

Berner, R.A., 1964. An idealized model of dissolved sulfate distribution in recent sediments. *Geochim. Cosmochim. Acta*, 28:1497–1503.

————, 1977. Stoichiometric models for nutrient regeneration in anoxic sediments. *Limnol. Oceanogr.*, 22:781–786.

————, 1980. *Early Diagenesis: A Theoretical Approach:* Princeton, NJ (Princeton Univ. Press).

Berner, U., and Koch, J., 1993. Organic matter in sediments of Site 808, Nankai Accretionary Prism, Japan. *In* Hill, I.A., Taira, A., Firth, J.V., et al., *Proc. ODP, Sci. Results*, 131: College Station, TX (Ocean Drilling Program), 379–385.

Blair, N.E., and Aller, R.C., 1995. Anaerobic methane oxidation on the Amazon shelf. *Geochim. Cosmochim. Acta*, 59:3707–3715.

Blair, N.E., Boehme, S.E., and Carter, W.D., 1993. The carbon isotope biogeochemistry of methane production in anoxic sediments, 1: field observations. *In* Oremland, R.S. (Ed.), *Biogeochemistry of Global Change*: New York (Chapman & Hall), 576–593.

Boehme, S.E., Blair, N.E., Chanton, J.P., and Martens, C.S., 1996. A mass balance of ^{13}C and ^{12}C in an organic-rich methane-producing sediment. *Geochim. Cosmochim. Acta*, 60:3835–3848.

Borowski, W.S., 1998. Pore-water sulfate concentration gradients, isotopic compositions, and diagenetic processes overlying continental margin, methane-rich sediments associated with gas hydrates [Ph.D. dissert.]. Univ.of North Carolina, Chapel Hill, NC.

Borowski, W.S., Paull, C.K., and Ussler, W., III, 1996. Marine pore-water sulfate profiles indicate in situ methane flux from underlying gas hydrate. *Geology*, 24:655–658.

Borowski, W.S., Paull, C.K., and Ussler, W., III, 1997. Carbon cycling within the upper methanogenic zone of continental rise sediments: an example from the methane-rich sediments overlying the Blake Ridge fas hydrate deposits. *Mar. Chem.*, 57:299–311.

Brooks, J.M., Bernard, L.A., Weisenburg, D.A., Kennicutt, M.C., II, and Kvenvolden, K.A., 1983. Molecular and isotopic compositions of hydrocarbons at Site 533, Deep Sea Drilling Project Leg 76. *In* Sheridan, R.E., Gradstein, F.M., et al., *Init. Repts. DSDP*, 76: Washington (U.S. Govt. Printing Office), 377–389.

Brown, F.S., Maedecker, M.J., Nissenbaum, A., and Kaplan, I.R., 1972. Early diagenesis in a reducing fjord, Saanich Inlet, British Columbia, III: Changes in organic constituents of sediment. *Geochim. Cosmochim. Acta,* 36:1185–1203.

Canfield, D.E., and Thamdrup, B., 1994. The production of ^{34}S-depleted sulfide during bacterial disproportionation of elemental sulfur. *Science,* 266:1973–1975.

Chambers, L.A., and Trudinger, P.A., 1979. Microbiological fractionation of stable sulfur isotopes: a review and critique. *Geomicrobiol. J.,* 1:249–293.

Claypool, G.E., and Threlkeld, C.N., 1983. Anoxic diagenesis and methane generation in sediments of the Blake Outer Ridge, Deep Sea Drilling Project Site 533, Leg 76. *In* Sheridan, R.E., Gradstein, F.M., et al., *Init. Repts. DSDP,* 76: Washington (U.S. Govt. Printing Office), 391–402.

Cragg, B.A., Parkes, R.J., Fry, J.C., Weightman, A.J., Rochelle, P.A., Maxwell, J.R., Kastner, M., Hovland, M., Whiticar, M.J., and Sample, J.C., 1995. The impact of fluid and gas venting on bacterial populations and processes in sediments from the Cascadia Margin accretionary system (Sites 888–892) and the geochemical consequences. *In* Carson, B., Westbrook, G.K., Musgrave, R.J., and Suess, E. (Eds.), *Proc. ODP, Sci. Results,* 146 (Pt. 1): College Station, TX (Ocean Drilling Program), 399-411.

Craig, H., 1953. The geochemistry of the stable carbon isotopes. *Geochim. Cosmochim. Acta,* 3:53–92.

Crill, P.M., and Martens, C.S., 1987. Biogeochemical cycling in an organic-rich coastal marine basin, 6: temporal and spatial variations in sulfate reduction rates. *Geochim. Cosmochim. Acta,* 51:1175–1186.

Davidson, C.W., Leaist, D.G., and Hesse, R., 1983, Oxygen-18 enrichment in the water of a clathrate hydrate. *Geochim. Cosmochim. Acta,* 47:2293–2295.

Deines, P., 1980. The isotopic composition of reduced organic carbon. *In* Fritz, P., and Fontes, J.C. (Eds.), *Handbook of Environmental Isotope Geochemistry* (Vol. 1)*: The Terrestrial Environment, A:* Amsterdam (Elsevier), 329–406.

Devol, A.H., 1983. Methane oxidation rates in the anaerobic sediments of Saanich Inlet. *Limnol. Oceanogr.,* 28:738–742.

Devol, A.H., and Ahmed, S.I., 1981. Are high rates of sulphate reduction associated with anaerobic oxidation of methane? *Nature,* 291:407–408.

Devol, A.H., Anderson, J.J., Kuivila, K., and Murray, J.W., 1984. A model for coupled sulfate reduction and methane oxidation in the sediments of Saanich Inlet. *Geochim. Cosmochim. Acta,* 48:993–1004.

Dillon, W.P., and Paull, C.K., 1983. Marine gas hydrates, II. Geophysical evidence. *In* Cox, J.L. (Ed.), *Natural Gas Hydrates: Properties, Occurrences, and Recovery:* Woburn, MA (Butterworth), 73–90.

Elsgaard, L., and Jorgensen, B.B., 1992. Anoxic transformations of radiolabeled hydrogen sulfide in marine and freshwater sediments. *Geochim. Cosmochim. Acta,* 56:2425–2435.

Emrich, K., Ehhalt, D., and Vogel, J., 1970. Carbon isotope fractionation during the precipitation of calcium carbonate. *Earth Planet. Sci. Lett.,* 8:363–371.

Fossing, H., and Jørgensen, B.B., 1990. Oxidation and reduction of radiolabeled inorganic sulphur compounds in an estuarine sediment, Kysing Fjord, Denmark. *Geochim. Cosmochim. Acta,* 54:2731–2742.

Fry, B., Jannasch, H.W., Molyneaux, S.J., Wirsen, C.O., Muramoto, J.A., and King, S., 1991. Stable isotope studies of the carbon, nitrogen and sulfur cycles in the Black Sea and the Cariaco Trench. *Deep-Sea Res.,* 38:1003–1019.

Galimov, E.M., and Kvenvolden, K.A., 1983. Concentrations of carbon isotopic compositions of CH_4 and CO_2 in gas from sediments of the Blake Outer Ridge, Deep Sea Drilling Project Leg 76. *In* Sheridan R.E., Gradstein, F.M., et al., *Init. Repts. DSDP,* 76: Washington (U.S. Govt. Printing Office), 403–407.

Gamo, T., Kastner, M., Berner, U., and Gieskes, J., 1993. Carbon isotope ratio of total inorganic carbon in pore waters associated with diagenesis of organic material at Site 808, Nankai Trough. *In* Hill, I.A., Taira, A., Firth, J.V., et al., *Proc. ODP, Sci. Results,* 131: College Station, TX (Ocean Drilling Program), 159–163.

Gieskes, J.M., Gamo, T., and Brumsack, H., 1991. Chemical methods for interstitial water analysis aboard *JOIDES Resolution. ODP Tech. Note,* 15.

Goldhaber, M.B., and Kaplan, I.R., 1974. The sulfur cycle. *In* Goldberg, E.D. (Ed.), *The Sea* (Vol. 5): *Marine Chemistry: The Sedimentary Cycle:* New York (Wiley-Interscience), 569–655.

Hesse, R., and Harrison, W.E., 1981. Gas hydrates (clathrates) causing pore-water freshening and oxygen isotope fractionation in deep-water sedimentary sections of terrigenous continental margins. *Earth Planet. Sci. Lett.,* 55:453–462.

Hoehler, T.M., Alperin, M.J., Albert, D.B., and Martens, C.S., 1994. Field and laboratory studies of methane oxidation in anoxic marine sediment: Evidence for a methanogen-sulfate reducer consortium. *Global Biogeochem. Cycles,* 8:451–463.

Hollister, C.D., Ewing, J.I., et al., 1972. *Init. Repts. DSDP,* 11: Washington (U.S. Govt. Printing Office).

Holt, B.D., and Engelkemeir, A.G., 1970. Thermal decomposition of barium sulfate to sulfur dioxide for mass spectrometric analysis. *Anal. Chem.,* 42:1451–1453.

Iversen, N., and Blackburn, T.H., 1981. Seasonal rates of methane oxidation in anoxic marine sediments. *Appl. Environ. Microbiol.,* 41:1295–1300.

Iversen, N., and Jørgensen, B.B., 1985. Anaerobic methane oxidation rates at the sulfate-methane transition in marine sediments from Kattegat and Skagerrak (Denmark). *Limnol. Oceanogr.,* 30:944–955.

Jenden, P.D., and Gieskes, J.M., 1983. Chemical and isotopic composition of interstitial water from Deep Sea Drilling Project Sites 533 and 534. *In* Sheridan, R.E., Gradstein, F.M., et al., *Init. Repts. DSDP,* 76: Washington (U.S. Govt. Printing Office), 453–461.

Kosiur, D.R., and Warford, A.L., 1979. Methane production and oxidation in Santa Barbara Basin sediments. *Estuarine Coastal Shelf Sci.,* 8:379–385.

Kvenvolden, K.A., and McDonald, T.J., 1985. Gas hydrates of the Middle America Trench—Deep Sea Drilling Project Leg 84. *In* von Huene, R., Aubouin, J., et al., *Init. Repts. DSDP,* 84: Washington (U.S. Govt. Printing Office), 667–682.

Lancelot, Y., and Ewing, J.I., 1972. Correlation of natural gas zonation and carbonate diagenesis in Tertiary sediments from the north-west Atlantic. *In* Hollister, C.D., Ewing, J.I., et al., *Init. Repts. DSDP,* 11: Washington (U.S. Govt. Printing Office), 791–799.

Lerman, A., 1979. *Geochemical Processes: Water and Sediment Environments*: New York (John Wiley and Sons).

Li, Y., and Gregory, S., 1974. Diffusion of ions in sea water and in deep-sea sediments. *Geochim. Cosmochim. Acta,* 38:703–714.

Manheim, F.T., 1966. A hydraulic squeezer for obtaining interstitial waters from consolidated and unconsolidated sediments. *Geol. Surv. Prof. Pap. U.S.,* 550-C:256–261.

Manheim, F.T., and Sayles, F.L., 1974. Composition and origin of interstitial waters of marine sediments, based on deep sea drill cores. *In* Goldberg, E.D. (Ed.), *The Sea* (Vol. 5): *Marine Chemistry: The Sedimentary Cycle:* New York (Wiley), 527–568.

Martens, C.S., and Berner, R.A., 1974. Methane production in the interstitial waters of sulfate-depleted marine sediments. *Science,* 185:1167–1169.

————, 1977. Interstitial water chemistry of anoxic Long Island Sound sediments. I. Dissolved gases. *Limnol. Oceanogr.,* 22:10–25.

Martens, C.S., and Klump, J.V., 1980. Biogeochemical cycling in an organic-rich coastal marine basin, I: methane sediment-water exchange processes. *Geochim. Cosmochim. Acta,* 44:471–490.

Masuzawa, T., Handa, N., Kitagawa, H., and Kusakabe, M., 1992. Sulfate reduction using methane in sediments beneath a bathyal “cold seep” giant clam community off Hatsushima Island, Sagami Bay, Japan. *Earth Planet. Sci. Lett.,* 110:39–50.

Murray, J.W., Grundmanis, V., and Smethie, W.M., 1978. Interstitial water chemistry in the sediments of Saanich Inlet. *Geochim. Cosmochim. Acta,* 42:1011–1026.

Niewohner, C., Henson, C., Kasten, S., Zabel, M., and Schultz, H.D., 1998. Deep sulfate reduction completely mediated by anaerobic methane oxidation in sediments of the upwelling area off Nambia. *Geochim. Cosmochim. Acta,* 62:455–464.

Nissenbaum, A., Presley, B.J., and Kaplan, I.R., 1972. Early diagenesis in a reducing fjord, Saanich Inlet, British Columbia, I: chemical and isotopic changes in major components of interstitial water. *Geochim. Cosmochim. Acta,* 36:1007–1027.

Olsen, K., 1997. Measurement of the δ^{13}C (org) and δ^{15}N (org) in sediments of the Blake Ridge, Ocean Drilling Program Leg 164 [Senior thesis]. Univ. of North Carolina, Chapel Hill, NC.

Paull, C.K., Matsumoto, R., Wallace, P.J., et al., 1996. *Proc. ODP, Init. Repts.,* 164: College Station, TX (Ocean Drilling Program).

Paull, C.K., Ussler, W., III, and Borowski, W.S., 1995. Methane-rich plumes on the Carolina continental rise: associations with gas hydrates. *Geology,* 23:8–92.

Presley, B.J., and Kaplan, I.R., 1972. Interstitial water chemistry: Deep Sea Drilling Project, Leg 11. *In* Hollister, C.D., Ewing, J.I., et al., *Init. Repts. DSDP,* 11: Washington (U.S. Govt. Printing Office), 1009–1012.

Presley, B.J., Petrowski, C., and Kaplan, I.R., 1973. Interstitial water chemistry, Deep Sea Drilling Project, Leg 10. *In* Worzel, J.L., Bryant, W., et al., *Init. Repts. DSDP,* 10: Washington (U.S. Govt. Printing Office), 613–614.

Reeburgh, W.S., 1976. Methane consumption in Cariaco Trench waters and sediments. *Earth Planet. Sci. Lett.,* 28:337–344.

————, 1980. Anaerobic methane oxidation: rate depth distribution in Skan Bay sediments. *Earth Planet. Sci. Lett.,* 47:345–352.

————, 1983. Rates of biogeochemical processes in anoxic sediments. *Annu. Rev. Earth Planet. Sci.,* 11:269–298.

Reeburgh, W.S., Ward, B.B., Whalen, S.C., Sandbeck, K.A., Kilpatrick, K.A., and Kerkhof, L.J., 1991. Black Sea methane geochemistry. *Deep-Sea Res.,* 38 (Suppl.2):S1189–S1210.

Rees, C.E., Jenkins, W.J., and Monster, J., 1978. The sulphur isotopic composition of ocean water sulphate. *Geochim. Cosmochim. Acta,* 42:377–381.

Richards, F.A., 1965. Anoxic basins and fjords. *In* Riley, J.P., and Skirrow, G. (Eds.), *Chemical Oceanography* (Vol. 1): New York (Academic Press), 611–645.

Rodriguez, N.M., Paull, C.K., and Borowski, W.S., 1997. Diagenetic zonation within gas-hydrate bearing sedimentary sections on the Blake Ridge, ODP Leg 164. *Trans. Am. Geophys. Union*, 78:F343. (Abstract)

Ruppel, C., 1997. Anomalously cold temperatures observed at the base of the gas hydrate stability zone on the U.S. Atlantic passive margin. *Geology,* 25:699–702.

Sayles, F.L., Manheim, F.T., and Waterman, L.S., 1972. Interstitial water studies on small core samples, Leg 11. *In* Hollister, C.D., Ewing, J.I., et al., *Init. Repts. DSDP,* 11: Washington (U.S. Govt. Printing Office), 997–1008.

Schulz, H.D., Dahmke, A., Schinzel, U., Wallmann, K., and Zabel, M., 1994. Early diagenetic processes, fluxes, and reaction rates in sediments of the South Atlantic. *Geochim. Cosmochim. Acta,* 58:2041–2060.

Sheridan, R.E., Gradstein, F.M., et al., 1983. *Init. Repts. DSDP,* 76: Washington (U.S. Govt. Printing Office).

Shipley, T.H., Houston, M.H., Buffler, R.T., Shaub, F.J., McMillen, K.J., Ladd, J.W., and Worzel, J.L., 1979. Seismic evidence for widespread possible gas hydrate horizons on continental slopes and rises. *AAPG Bull.,* 63:2204–2213.

Sorensen, J., and Jørgensen, B.B., 1987. Early diagenesis in sediments from Danish coastal waters: microbial activity and Mn-Fe-S geochemistry. *Geochim. Cosmochim. Acta,* 51:1583–1590.

Suess, E., and Whiticar, M.J., 1989. Methane-derived CO_2 in pore fluids expelled from the Oregon subduction zone. *Palaeogeogr., Palaeoclimatol., Palaeoecol.,* 71:119–136.

Thierstein, H.R., Geitzenauer, K., Molfino, B., and Shackleton, N.J., 1977. Global synchroneity of late Quaternary coccolith datum levels: validation by oxygen isotopes. *Geology,* 5:400–404.

Uchupi, E., 1968. Atlantic continental shelf and slope of the United States: physiography. *U.S. Geol. Surv. Prof. Pap.,* 529–C.

Ullman, W.J., and Aller, R.C., 1982. Diffusion coefficients in nearshore marine sediments. *Limnol. Oceanogr.,* 27:552–556.

von Breymann, M.T., Swart, P.K., Brass, G.W., and Berner, U., 1991. Porewater chemistry of the Sulu and Celebes Seas: extensive diagenetic reactions at Sites 767 and 768. *In* Silver, E.A., Rangin, C., von Breymann, M.T., et al., *Proc. ODP, Sci. Results,* 124: College Station, TX (Ocean Drilling Program), 203–215.

Vuletich, A.K., Threlkeld, C.N., and Claypool, G.E., 1989. Isotopic composition of gases and interstitial fluids in sediment of the Vøring Plateau, ODP Leg 104, Site 644. *In* Eldholm, O., Thiede, J., Taylor, E., et al., *Proc. ODP, Sci. Results,* 104: College Station, TX (Ocean Drilling Program), 281–283.

Whiticar, M.J., and Faber, E., 1986. Methane oxidation in sediment and water column environments: isotope evidence. *In* Leythaeuser, D., and Rullkötter, J. (Eds.), *Advances in Organic Geochemistry.* Org. Geochem., 10:759–768.

Whiticar, M.J., Hovland, M., Kastner, M., and Sample, J.C., 1995. Organic geochemistry of gases, fluids, and hydrates at the Cascadia accretionary margin. *In* Carson, B., Westbrook, G.K., Musgrave, R.J., and Suess, E. (Eds.), *Proc. ODP, Sci. Results,* 146 (Pt 1): College Station, TX (Ocean Drilling Program), 385–397.

Young, H.D., 1962. *Statistical Treatment of Experimental Data:* New York (McGraw-Hill).

Date of initial receipt: 21 April 1998
Date of acceptance: 12 January 1999
Ms 164SR-214

Table 4. Table showing marine localities (coastal and deep-sea sediments) where anaerobic methane oxidation (AMO) is an important process.

Location	Maximum AMO rate ($\mu mol\ cm^{-3}\ yr^{-1}$)	Method	Depth to SMI (mbsf)	Sulfate depletion due to AMO (%)	Lightest $\delta^{13}C$-$\Sigma C0_2$ (‰ PDB)	$\delta^{13}C$-organic matter (‰ PDB)	Reference
Coastal Marine:							
Amazon Shelf (OST-2)	—	Model CH_4	0.60-0.67	—	–29 (at SMI)	–22	Blair and Aller (1995)
Cape Lookout Bight (Coastal North Carolina)	70-510	Labeled S^*O_4	—	—	—	—	Crill and Martens (1987)
	—		0.05	—	–10 to –15 (at SMI)	—	Blair et al. (1993)
	2.9	Labeled C^*H_4	—	—	—	—	Alperin et al. (1992)
	4.4-5.5	Labeled C^*H_4	0.05-0.12	—	—	—	Hoehler et al. (1994)
	—	—	—	—	–5 to –15 (at SMI)	–19.2 ± 0.2	Boehme et al. (1996)
Kysing Fjord, Denmark	0.017-0.102	Labeled C^*H_4	0.01-0.05	0.01-0.06	—	—	Iversen and Blackburn (1981)
Jutland and Kuttegat, Denmark	2.0-4.0	Labeled C^*	0.2-1.3	10-17	—	—	Iversen and Jorgensen (1985)
	2-6.6	Labeled S^*O_4					
Long Island Sound	0.65	Model CH_4	0.15-0.80	—	—	—	Martens and Berner (1977)
Skan Bay, Alaska	1.8-3.4	Labeled C^*	0.18	5-20	–19 to –21 (at SMI)	–21	Reeburgh (1980)
	3.65	Labeled C^*H_4			—	—	Alperin and Reeburgh (1984)
	5-20	Labeled C^*H_4			—	—	Alperin et al. (1988)
	29	Labeled C^*H_4			—	—	Alperin et al. (1992)
Saanich Inlet, Vancouver	—	—	<0.15-0.30	—	—	–20 to –24	Brown et al. (1972)
	—	—	<0.10-0.85	—	–37.1 (near SMI)	—	Nissenbaum et al. (1972)
		Model SO_4	0.17-0.24	75	—	—	Murray et al. (1978)
	35-78	Labeled S^*O_4	0.17	30-70	—	—	Devol and Ahmed (1981)
	1.7-7	Labeled C^*H_4	—	—	—	—	Devol (1983)
	35-70	Labeled S^*O_4			—	—	
	2.6-6.6	Labeled C^*H_4	0.12	23-40	—	—	Devol et al. (1984)
	17-52	Labeled S^*O_4			—	—	
	30	Model CH_4			—	—	
	30	Model SO_4			—	—	
Santa Barbara Basin	0.232 (46 cm zone)	Model	0.90-2.1	—	—	—	Barnes and Goldberg (1976)
	0.128 (mean)	Labeled acetate	—	—	—	—	Kosiur and Warford (1979)
Deep Sea:							
Black Sea (BS5–10)	$(4.6\text{-}9.5) \times 10^{-4}$	Labeled C^*H_4	Anoxic water column	—	—	—	Reeburgh et al. (1991)
	—	—		—	—	–22 to –27	Fry et al. (1991)
Cariaco Trench	0.55-1.59	Model CH_4	0.55-0.70	50	—	—	Reeburgh (1976)
	(10 cm zone)	—	—	—	—	–19 to –21	Fry et al. (1991)
Gulf of Mexico (DSDP Site 88)	—	—	5-54	—	–30 (4 mbsf)	—	Presley et al. (1973)
Blake Ridge (DSDP Site 533)	—	—	9.8-14.4	—	–31.4 (14 mbsf)	—	Claypool and Threlkeld (1983)
Blake Ridge (ODP Site 995)	0.005	Model CH_4	20	~33	–37.7 (20 mbsf)	–21 (mean)	This paper
Norwegian Sea (ODP Site 644)	—	—	6-22	—	–31.8 (22 mbsf)	—	Vuletich et al. (1989)
Sulu Basin (ODP Site 768)	—	—	~172	—	–34 (172 mbsf)	—	von Breymann et al. (1991)
Nankai Trough	—	—	3-13.8	—	–29.8 (3 mbsf)	—	Gamo et al. (1993)
(ODP Site 808)	—	—	—	—	—	–23 to –25	Berner and Koch (1993)
Offshore Namibia	—	Flux calculation	3.5-10	40-100	—	—	Niewohner et al. (1998)

Note: * = radioisotopes. SMI = Sulfate/methane interface, PDB = Peedee belemnite standard. — = not measured.